



ELSEVIER

Physica E 2 (1998) 694–700

PHYSICA E

# Optical spectroscopy of a single self-assembled quantum dot

E. Dekel<sup>a,\*</sup>, D. Gershoni<sup>a</sup>, E. Ehrenfreund<sup>a</sup>, D. Spektor<sup>a</sup>, J.M. Garcia<sup>b</sup>, P.M. Petroff<sup>b</sup>

<sup>a</sup>*Department of Physics and Solid State Institute, Technion–Israel Institute of Technology, Haifa 32000, Israel*

<sup>b</sup>*University of California, Santa Barbara, CA 93106, USA*

---

## Abstract

We apply diffraction-limited confocal optical microscopy to spatially resolve, a *single* self-assembled semiconductor quantum dot. We report for the first time, on the low-temperature photoluminescence spectrum of such a single dot and on its excitation intensity dependence. We demonstrate that sharp spectral lines, in the dots emission spectrum, are due to optical transitions between discrete multiexcitonic states confined within the dot. Under high excitation power, once the limited number of discrete exciton levels are fully occupied, spectrally broad emission bands are formed due to transitions which involve continuum excitonic states. In addition, we show that the single exciton recombination is almost forbidden in this InAs self-assembled quantum dot. © 1998 Elsevier Science B.V. All rights reserved.

*Keywords:* Self-assembled quantum dots; Microphotoluminescence; Excitons in quantum dots

---

## 1. Introduction

The study of electronic processes in semiconductor heterostructures of reduced dimensionality has been a subject of recent extensive research efforts. Of particular importance are the efforts to fabricate and study semiconductor quantum dots (QDs) of nanometer size, in which the charge carriers are confined in all three directions to characteristic lengths which are smaller than their De Broglie wavelengths [1–21]. These efforts are motivated by both the QDs potential device applications as well as their being an excellent stage for experimental studies of basic quantum mechanical principles [21]. One very promising way of fabricating such QDs is the so-named self-assembled

QDs (SAQDs) method. This method uses the lattice mismatch strain between different epitaxially grown semiconductor layers for the formation of small islands connected by a very thin wetting layer. This deposition mode (named after Stranski and Krastanow) reduces the energy associated with the lattice mismatch strain of the epitaxial deposition. By capping these self-assembled islands with an epitaxial layer of higher-energy band gap and lattice constant which is similar to that of the substrate, high-quality QDs can be produced [8,9,22]. This relatively simple way of producing large ensembles of QDs has motivated a vast number of studies of these dots and their electronic and optical properties [8,9,22–27]. The size distribution of the SAQDs (typically about 10%), and the resultant inhomogeneous broadening of the SAQDs ensemble spectral features, has so far limited

\* Corresponding author. E-mail: sserez@ssrc.technion.ac.il.

the ability to clearly understand and unambiguously interpret the experimental results.

In this work, we overcome this experimental obstacle, by spectroscopically studying for the first time, multiexcitonic optical transitions in such a *single* SAQD. We show here, indeed, that multiple sharp spectral lines, as well as broad spectral features, which previously were always interpreted as an optical signature for emission from an ensemble of dots [8,9], can actually be a result of carrier recombination within a single dot, under various excitation levels.

## 2. Experimental

The SAQD sample that we studied optically was fabricated by deposition of a defect free coherently strained epitaxial layer of InAs on an AlGaAs layer lattice-matched to GaAs substrate. The layer sequence, compositions and widths are given in the inset to Fig. 1. These high-quality QDs, have large confining potentials for carriers and a well-demonstrated zero-dimensionality character [9,23,24]. The use of AlGaAs as the cladding material for these SAQDs made them to efficiently emit in the near-infrared range, at wavelength which is detectable by silicon-based detectors, and thus form an excellent stage for performing low light level spectroscopy which is required for the studies of a single quantum dot. The low-temperature far-field photoluminescence (PL) spectrum of the SAQDs sample is displayed in Fig. 1. During the growth of the strained layer, the sample was not rotated, thus a gradient in the QDs density was formed across its surface [23]. In particular, low-density areas, in which the average distance between neighboring QDs is comparable and larger than our spatial resolution ( $< 1 \mu\text{m}$ ) could easily be found on the sample surface. We use diffraction limited low temperature confocal optical microscope for the photoluminescence (PL) studies of the single SAQDs. The setup is schematically described in the inset to Fig. 2. We use a  $\times 100$  in situ microscope objective and a CCD-camera-based active feedback loop for stabilizing the microscope–sample working distance. Our system provides diffraction limited spatial resolution, both in the excitation and the detection channels. We have tested the combined spatial resolution of our system by creating selective PL images of a cleaved

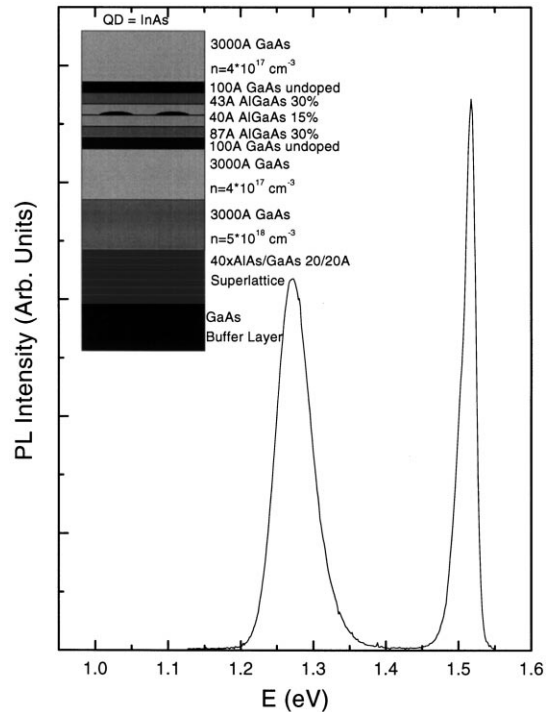


Fig. 1. Far-field low-temperature photoluminescence spectrum of the self-assembled dots sample. The inset describes the sample layers sequence.

edge of a single quantum well (SQW) sample [28]. The spatial full width at half maximum of the SQW PL emission intensity was found to be 0.5–0.6  $\mu\text{m}$ , in agreement with the expected diffraction limited optical resolution at this wavelength ( $\approx 750 \text{ nm}$ ).

## 3. Results

The dots position and characteristic emission wavelength are found by taking PL line scans over the SAQD sample surface. A typical such line scan is displayed in Fig. 2, where the PL intensity as a function of photon energy and objective position is given by the gray color scale as indicated by the color bar in the figure. During this line scan, the PL was excited with a  $7 \mu\text{W}$  cw light from a titanium sapphire laser at wavelength of 730 nm. The microscope objective was moved in steps of  $0.1 \mu\text{m}$ , in each of which the PL spectrum was measured by exposing a liquid nitrogen cooled CCD camera for 50 s. Three

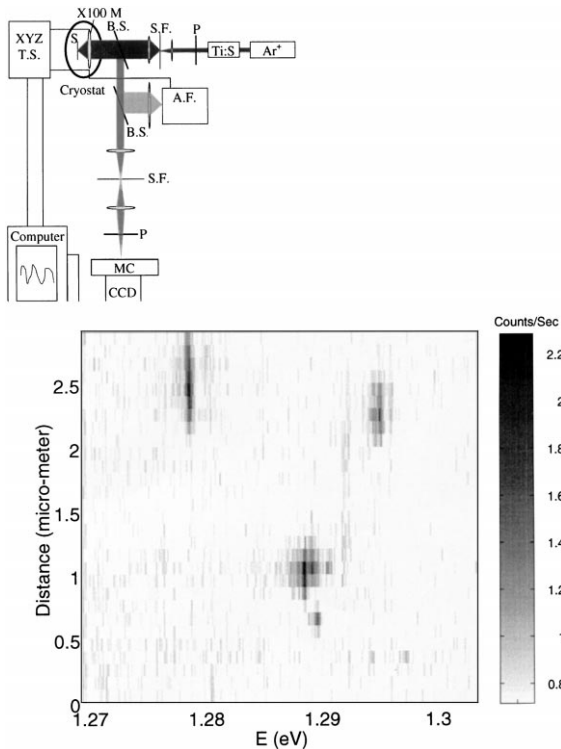


Fig. 2. PL emission intensity as a function of photon energy and position along a  $3\ \mu\text{m}$  line scan across the SAQD sample surface. The PL intensity is given by the gray color scale as indicated by the bar to the right. The inset presents a schematic description of the low temperature diffraction limited confocal scanning optical microscope setup. The X100 Microscope (M) lens is placed inside the cryostat near the sample (S) on an XYZ translation stage (TS) which is controlled by an auto-focus (AF) feedback system. SF-spatial filter, BS-beam splitter, P-polarizer, MC-monochromator, CCD-charge coupled device camera.

emission lines from three different spatial positions along the scanned line are evident in Fig. 2. These lines are due to recombination of excitons within a single SAQD, as indicated by their spatial and spectral widths, which are both resolution limited [14,29]. In Fig. 3 we present PL spectra from a single SAQD for various excitation powers. The spectra are vertically displayed for clarity, and the zero for each spectrum is represented by a short horizontal line to the left of the figure. The spatial position of the dot was found by a line scan procedure as explained above, and exposure times of 50 s were used in obtaining the experimental data. The observed spectra are very sensi-

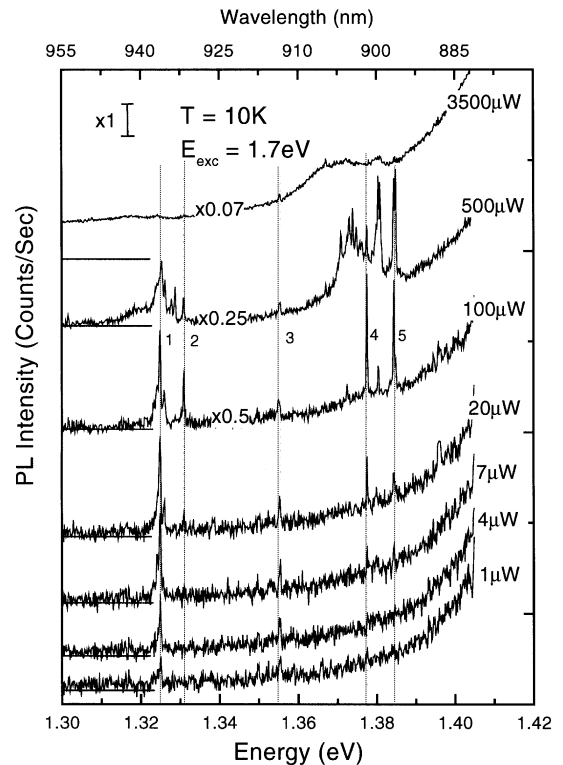


Fig. 3. PL spectra from a single SAQD for various excitation power levels.

tive to the excitation power, as expected for a finite size dot, where the degeneracy of the quantum states is limited to a small finite number. An overall perception of the optical transitions between the discrete excitonic states of the dot can be obtained from the spectrum at  $100\ \mu\text{W}$  excitation power. This spectrum is composed of two groups of emission lines separated by  $\approx 50\ \text{meV}$ . The two groups are located near 1.325 and 1.375 eV, respectively, with spectral symmetry about a central weak emission line at 1.355 eV. Each group is composed of several sharp and well-resolved lines, two of which, roughly 7 meV apart, are particularly strong. For the sake of the following discussion, we marked the strongest line in each group and the center line by numbers from 1 to 5 in increasing order according to their spectral position. At excitation power of  $1\ \mu\text{W}$ , only lines 1 and 3 are observed. The measured emission intensity of these lines, at these low excitation powers, is lower than one count per

second. We believe that this is a result of the low efficiency of our high spatial resolution collection optics. The excitation power dependence of these two lines is very different. The emission of line No. 1 increases roughly as the square root of the excitation power up to about  $100 \mu\text{W}$ , where it reaches saturation. Line No. 3, on the other hand, reaches saturation already at excitation power of  $7 \mu\text{W}$ , where its emission rate is roughly one-quarter of that of line No. 1, which starts to develop small satellites from both its sides. As the power increases to  $20 \mu\text{W}$  the emission spectrum is composed of all five main spectral lines, and two other small lines, in between lines Nos. 1 and 2, and lines Nos. 4 and 5, respectively. Upon increasing the excitation power of  $100 \mu\text{W}$ , all four main lines reach saturation. Their emission rate is now roughly an order of magnitude larger than the emission rate of the saturated, mid energy line No. 3, except for line No. 2 which has roughly half the intensity of lines 1, 4 and 5. As the excitation power further increases above  $100 \mu\text{W}$ , broad bands below each group of lines are becoming the dominant spectral features and the spectrum eventually loses its discrete nature.

#### 4. Discussion

For a qualitative analysis of our observations we use a model rectangular dot, with base dimensions of  $30 \times 30 \text{ nm}^2$  and height of  $5 \text{ nm}$ . The finite barrier height of our model dot allow for only two confined electronic levels within the dot. Since we are interested in neutral states, only two hole levels are considered as well. The energy levels are schematically described in the inset of Fig. 4. Due to spin, the first single carrier level is doubly degenerate, and due to the equivalency between the two directions which are perpendicular to the growth axis (the height of the SAQD), the second level of the SAQD is four time degenerate [30]. Our model dot may not accurately describe the SAQD potential structure since an SAQD has different geometrical shape [22], and the model does not take into account the presence of strain and piezoelectric fields within the SAQD [32]. We still expect our model to at least partially explain our experimental data, since the properties of a fully quantized system should be, to a large degree, independent of the details of its confining

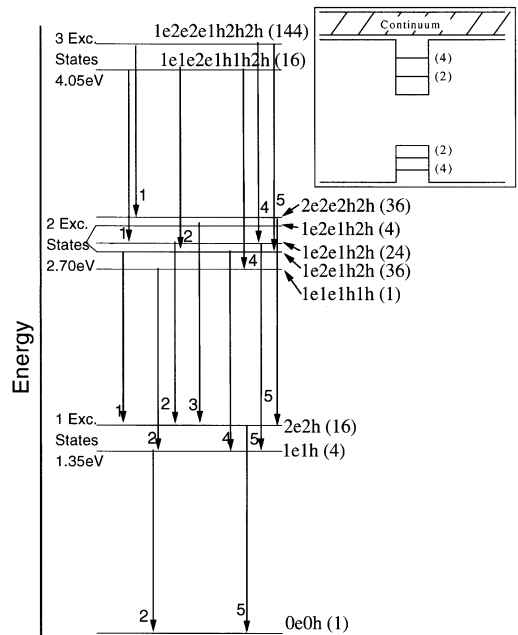


Fig. 4. Schematic description of the main optical transitions between the quantum dot multiexciton states. For simplicity, only the first 4 out of 7 multiexciton states are presented. From symmetry considerations it is clear, that these are enough to explain the main 5 spectral lines that were experimentally observed.

potentials. As we show below, the important features of our model, are its number of discrete electronic levels and their degeneracies. We understand our observations in terms of optical transitions between multiexcitonic states in the SAQD. These optical transitions are schematically described in Fig. 4. In the figure the vertical lines represent the multiexcitonic levels and vertical arrows represent the optical transitions. The ground no exciton state and the next three multiexcitonic states are represented in the figure. As can be seen in the figure, more than one excitonic level is available for each multiexcitonic state, depending on the particular arrangement of the energy levels of electrons and holes which compose the multiexcitonic state. These arrangements are indicated by the level index of the participating charge particles, to the right of each level. The indices e and h stand for electron and hole, respectively. The levels are highly degenerate, as indicated by the bracketed numbers to the side of each level. In the diagram we have not listed all the levels within each multiexcitonic state.

For the sake of simplicity, we present in our figure only the levels which are relevant to the main optical transitions that we observed. A more thorough theoretical treatment (though of a geometrically different dot) can be found in Ref. [31]. All but one multiexcitonic level in our scheme (the biexcitonic level  $1e2e1h2h$ ) are essentially described by their parent, single charge carriers levels. This is due to the effect of the Coulomb interaction, between diagonal neutral states, which amounts only to a rigid energy shift of the single carrier level and no degeneracy is lifted [31]. The degeneracy of the 64  $1e2e1h2h$  biexcitonic states is lifted by the nondiagonal Coulomb interaction term in a similar way to a bulk biexciton [32]. The relative intensity of the optically allowed transitions between the multiexcitonic levels can now be quite straightforwardly estimated if one takes into account the degeneracy of the initial state, final state and the fact that an interband optical transition is only allowed between states of the same total spin, the same spin projection on the growth axis, and the same parity. (We assumed here that the overlap integrals between the single charge carriers envelope wave function is of order unity.) We marked the optical transitions by numbers 1–5 in order of increasing energy.

By comparing our data with the dot model calculations one can deduce that the  $\approx 52$  meV separation between the two groups of lines corresponds to the energy difference between the lowest quantized single-exciton state (which is composed of an electron and a hole in their lowest-energy states) and the upper-most single-exciton state (which is composed of an electron and a hole in their second energy level), respectively. The optical transitions from these two optically active single-exciton states to the no-exciton states are represented by line Nos. 2 and 5, respectively. The energy separation between these excitonic transitions is compatible with quantization dimensions of 30 nm, which are typical to these SAQDs [23]. Lines Nos. 1 and 4, can only result from optical transitions between multiexcitonic states, as clearly demonstrated in Fig. 4. These lines, which are red-shifted by 7 meV relative to lines Nos. 2 and 5, are due to optical transitions between the highest degeneracy biexcitonic state  $1e2e1h2h$  and the excitonic states  $2e2h$  and  $1e1h$ , respectively. The energy separation between line Nos. 1 and 2 and line Nos. 4 and 5 is a direct measure of the off-diagonal elements of the Coulomb interaction be-

tween the single-particle states. This interaction mixes charged particle states of different quantum numbers and allows for optical transitions between multiexciton states of different electron and hole quantum numbers. The 7 meV shift that we measure agrees well with our model calculations. Line No. 3 is readily understood as a biexciton–exciton optical transition, as shown in Fig. 4. Its relatively small oscillator strength agrees well with the experimental measurements. The fact that the energy separation between line Nos. 2 and 3 (22 meV) is more than three times larger than the separation between line Nos. 1 and 2 is not revealed by our dot model calculations and we believe that it has to do with the details of the dot structure.

The observation of two energetically symmetrical group of lines is a clear indication that our SAQD has only two discrete electron confined states. This conclusion is in agreement with Ref. [9], where two electronic levels were clearly observed by capacitance measurements.

The intensity of the various spectral lines that we observe and their excitation power dependence can also be understood by inspection of Fig. 4. Using conservative estimates of the reflection from the sample surface and the absorption within the different sample layers, we find that the average number of excitons, within the SAQD, is roughly given by  $3I_L\tau$ , where  $I_L$  is the excitation power in  $\mu\text{W}$  and  $\tau$  is the excited species lifetime in nanoseconds. Thus, for an excitation power of  $I_L = 1 \mu\text{W}$  and exciton lifetime of  $\tau = 500$  ps [24], more than one exciton can be found at the SAQD on average at any given time. As the excitation power increases, this number increases. However, this increase is not linear in power, since higher-energy states have more decay channels and consequently shorter lifetimes [27].

The assumption that at excitation power of  $\approx 1 \mu\text{W}$  more than one exciton is present in the SAQD on average can also be safely deduced from the emission spectrum. Since the intensity of line No. 3 originates only from an optical transition between biexciton to single exciton in the dot (see Fig. 4), its saturation is a clear indication for the average presence of two excitons within the SAQD at any given time. At this excitation power (7–10  $\mu\text{W}$ ), line No. 1 should be four times stronger than the saturated line No. 3. This is in agreement with our measurements (see Fig. 3). Line No. 1 is not saturated at this excitation power,

since optical transitions from tri- to biexcitons and from higher multiexcitonic states also contribute to its strength.

If we assume full thermalization between the two quantized electronic levels in the dot, which are separated in energy by more than the energy of an optical phonon [9,34,35], the first doubly degenerate electronic level is completely full when two excitons on average are present in the SAQD. Thus, higher excitation power will result in population of the second quantized electronic level, and a rapid increase in the emission intensity of the higher-energy group of spectral lines. Concurrently, the low-energy group only doubles its strength before reaching saturation. This is exactly what we observe. At complete saturation of the initial set of discrete lines (50–100  $\mu\text{W}$ ) we measure 1:10 ratio between the saturated mid-energy PL line and the saturated lowest-energy line. This is in agreement with the calculated sum of all the allowed optical transitions. Lines Nos. 4 and 5 are about a factor of two stronger than line No. 1, in agreement with our calculations, due to the two-fold “geometrical” degeneracy of the second quantum level in the SAQD. Since the higher-energy level contains twice as many excitons as the lower one, emission lines which originate from this level are about a factor of two stronger than those originate from the lowest level.

Yet higher excitation power results in more than 6 excitons in average within the SAQD. These excitons occupy continuum states (see inset of Fig. 4). Optical transitions originating from these multiexcitonic states result in broad and smooth emission lines to the lower-energy side of each group of discrete spectral lines.

If we assume that recombination is possible only via radiative channels it follows that the lifetime of the biexciton state in a dot, is roughly comparable to the lifetime of the triexciton states and few times faster than the single exciton lifetime. Now, since the degeneracy of the second level is twice the degeneracy of the first level, a four-fold increase in the power is required in order to reach a complete saturation of the second electronic level of the dot. At this point, all the dot discrete electronic levels are full, two electrons occupy the ground level and four electrons occupy the second energy level of the SAQD. The estimate of four-fold increase in excitation power from the power required to generate average population of two exci-

tons in the SAQD to the power required to generate six excitons in the SAQD is comparable but somewhat lower than what we measure (6–8). This might be a consequence of the somewhat rough assumption that the lifetimes of all the multiexcitonic states (2–6) are equal.

Before concluding, we note that line No. 2, which corresponds to the recombination of a single exciton state, is not observed at all at the low excitation power spectra. This line, at 1.331 eV, starts to be observable only after the first electronic level is full (the 20  $\mu\text{W}$  excitation spectrum). The line is also saturated at emission rates which are significantly lower than our calculated sum of allowed optical transitions. We believe that this is a consequence of the different shapes of the confining potentials for the electrons and for the holes, due to the strain and piezoelectric field [33]. The piezoelectric field reduces the overlap integral between the two charged particles and reduces their radiative recombination rate considerably. Only in the presence of two electron–hole pairs, this field is screened and higher multiexcitonic transitions are becoming allowed. Another possible explanation is that the lowest excitonic state is dark due to the exchange interaction which should amount to a few meV in these SQAD [36]. Similar effect was observed in II–VI nanocrystallites [18]. Thus, the biexciton lines No. 1 and 3 are the first to be observed and not the single-exciton line No. 2.

In conclusion, we have measured the low-temperature emission spectra of a single self-assembled semiconductor quantum dot, on a wide range of level occupation. We interpret our observations in terms of shell fillings of quantized multiexcitonic states within the dot. By close comparison with a simple theoretical model we understand well the observed sharp emission multi line spectrum and its excitation power dependence. We clearly demonstrate that the single-exciton transition is optically forbidden in these dots, and that the observed lowest excitation power emission line originates from a multiexcitonic state. At successively higher excitation power, we observe multiexciton state filling up to 6 confined excitons within the SQAD. At yet higher excitation powers, optical transitions which involve continuum electronic states are observed and the emission spectra from the single dot lose their discrete sharp nature.

## Acknowledgements

The work at the Technion was supported by the Israel Science Foundation. J.M.G. acknowledges the support of the Spanish Ministry of Science and Education.

## References

- [1] L.E. Brus, *J. Chem. Phys.* 79 (1983) 5566.
- [2] M.A. Reed, J.N. Randall, R.J. Aggarwal, R.J. Matyi, T.M. Moore, A.E. Wetsel, *Phys. Rev. Lett.* 60 (1988) 535.
- [3] H. Temkin, G.J. Dolan, M.B. Panish, S.N.G. Chu, *Appl. Phys. Lett.* 50 (1987) 413.
- [4] P.L. McEuen et al., *Phys. Rev. Lett.* 66 (1991) 1926.
- [5] C.W. Sneyder, B.G. Orr, D. Kessler, L.M. Sander, *Phys. Rev. Lett.* 66 (1991) 3032.
- [6] K. Brunner, U. Bockelmann, G. Abstreiter, M. Walther, G. Böhm, G. Trankle, G. Weimann, *Phys. Rev. Lett.* 69 (1992) 3216.
- [7] J. Tersoff, R.M. Tromp, *Phys. Rev. Lett.* 70 (1993) 2782.
- [8] J.-Y. Marzin, J.-M. Gerard, A. Izrael, D. Barrier, G. Bastard, *Phys. Rev. Lett.* 73 (1994) 716.
- [9] H. Drexler, D. Leonard, W. Hansen, J.P. Kotthaus, P.M. Petroff, *Phys. Rev. Lett.* 73 (1994) 2252.
- [10] K. Brunner, G. Abstreiter, G. Böhm, G. Trankle, G. Weimann, *Phys. Rev. Lett.* 73 (1994) 1138.
- [11] A. Zrenner, L.V. Butov, M. Hagan, G. Abstreiter, G. Böhm, G. Weimann, *Phys. Rev. Lett.* 72 (1994) 3382.
- [12] R. Strenz, U. Bockelmann, F. Hirler, G. Abstreiter, G. Böhm, G. Weimann, *Phys. Rev. Lett.* 73 (1994) 3022.
- [13] M. Nirmal et al., *Phys. Rev. Lett.* 75 (1995) 3728.
- [14] D. Gammon, E.S. Snow, B.V. Shanabrook, D.S. Katzer, D. Park, *Phys. Rev. Lett.* 76 (1996) 3005.
- [15] D. Gammon, E.S. Snow, B.V. Shanabrook, D.S. Katzer, D. Park, *Science* 273 (1996) 87.
- [16] S. Tarucha, D.G. Austing, T. Honda, R.J. van der Hage, L.P. Kouwenhoven, *Phys. Rev. Lett.* 77 (1996) 3613.
- [17] U. Bockelmann, Ph. Roussignol, A. Filoramo, W. Heller, G. Abstreiter, K. Brunner, G. Böhm, G. Weimann, *Phys. Rev. Lett.* 76 (1996) 3622.
- [18] S.A. Empedocles, D.J. Norris, M.G. Bawendi, *Phys. Rev. Lett.* 77 (1996) 3873.
- [19] Al.L. Efros, M. Rosen, *Phys. Rev. Lett.* 78 (1997) 1110.
- [20] W. Wegscheider, G. Schedelbeck, G. Abstreiter, M. Rother, M. Bichler, *Phys. Rev. Lett.* 79 (1997) 1917.
- [21] For a review see in: C. Weisbuch, E. Burstein (Eds.), *Confined Electrons and Photons*, NATO ASI Series, Plenum, New York, 1995.
- [22] D. Leonard, P.M. Petroff et al., *Phys. Rev. B* 50 (1994) 8086.
- [23] S. Fafard, R. Leon, D. Leonard, J.L. Merz, P.M. Petroff, *Phys. Rev. B* 52 (1995) 5752.
- [24] S. Raymond, S. Fafard, P.J. Poole, A. Wojs, P. Hawrylak, S. Charbonneau, D. Leonard, R. Leon, P.M. Petroff, J.L. Merz, *Phys. Rev. B* 54 (1996) 11 548.
- [25] M. Grundmann, J. Christen, N.N. Ledentsov et al., *Phys. Rev. Lett.* 74 (1995) 4043.
- [26] V.A. Shchukin, N.N. Ledentsov, P.S. Kopev, D. Bimberg, *Phys. Rev. Lett.* 75 (1995) 2968.
- [27] S. Grosse, J.H.H. Sandman, G. von Plessen, J. Feldman, H. Lipsanen, M. Sopanen, J. Tulkki, J. Ahopelto, *Phys. Rev. B* 55 (1997) 4473.
- [28] T.D. Harris, D. Gershoni, R.D. Grober, L.N. Pfeiffer, K.W. West, N. Chand, *Appl. Phys. Lett.* 68 (1996) 988.
- [29] H.F. Hess, E. Betzig, T.D. Harris, L.N. Pfeiffer, K.W. West, *Science* 264 (1994) 1740.
- [30] A. Wojs, P. Hawrylak, *Phys. Rev. B* 53 (1996) 10 841.
- [31] A. Barenco, M.A. Dupertuis, *Phys. Rev. B* 52 (1995) 2766.
- [32] J.J. Forney, A. Quattropani, F. Bassani, *Nuovo Cimento B* 22 (1974) 153.
- [33] C. Pryor, M.-E. Pistol, L. Samuelson, *Phys. Rev. B* 56 (1997) 10404.
- [34] H. Benisty, C.M. Sotomayor-Torres, C. Weisbuch, *Phys. Rev. B* 44 (1991) 10945.
- [35] H. Benisty, *Phys. Rev. B* 51 (1995) 13 281.
- [36] A. Franceschetti, A. Zunger, *Phys. Rev. Lett.* 78 (1997) 917.